

occur as isolated individuals, no preferred orientation is observed with respect to crystallographic directions of the substrate carbonate (Fig. 1B) or pyroxene (Fig. 3B). Moreover, changing the viewing angle shows that they are not rooted in specific planes of the substrate minerals.

Further information on the rod-shaped forms can be inferred from EDS chemical analysis. The chemical composition of an individual rod cannot be determined directly because it is too small for EDS techniques. However, for the clusters with sizes of a few micrometers, a qualitative analysis is made possible. The inferred composition of the clusters is indistinguishable from that of the substrate calcite. The rods are thus either purely inorganic calcite-rich precipitates or mineralized organisms. Chemical analyses confirm that they cannot be magnetite or other iron oxides, iron hydroxides, or silicates. Similar forms 5 to 10 times larger are conventionally interpreted to be bacterial relicts (11). Although, there is no direct evidence for bacterial activity, we note that, in addition to the rod-shaped forms and their surface textures (Fig. 1D), there is an intimate association between the saucer-shaped

depression in the pyroxene and the carbonates. The observed depressions could result from bacteria exploiting the immediate presence of chemical elements—carbon and calcium from the carbonates, and iron, silicon, and so forth from the orthopyroxenes.

We propose the following scenario for Tatahouine's residence on Earth. In 1931, the meteorite fell and was found with unfilled fractures. During the 63-year history of the meteorite in the desert soil, fluids transferred carbonates from the local sediments or soil to the meteorite, filling the preexisting fractures and locally coating the fragment surfaces. This demonstrates that meteorites can acquire terrestrial minerals in a very short time.

#### REFERENCES AND NOTES

1. A. Lacroix, *C. R. Acad. Sci. Paris* **193**, 305 (1931).
2. R. N. Clayton and T. K. Mayeda, *Geochim. Cosmochim. Acta* **60**, 1999 (1996).
3. The Raman data were collected with a DILOR XY micro-Raman spectrometer. A 100× objective was used to focus the beam of an argon laser ( $\lambda = 514.5$  nm) to give a spot of 2  $\mu\text{m}$  on the sample.
4. M. Zolensky and H. Y. McSweeney Jr., in *Meteorites and the Early Solar System*, J. F. Kerridge and M. S. Matthews, Eds. (Univ. of Arizona Press, Tucson, AZ, 1988), pp. 114–143; D. W. Mittlefehldt, *Meteoritics* **29**, 214 (1994); J. L. Gooding, S. J. Wentworth, M. E. Zolensky, *Geochim. Cosmochim. Acta* **52**, 909 (1988); B. Mason *et al.*, *Smithson. Contrib. Earth Sci.* **30**, 17 (1992); A. J. T. Jull, C. J. Eastoe, S. Cloudf, *J. Geophys. Res.* **102**, 1663 (1997).
5. Isotopic analyses were performed on  $\text{CO}_2$  gas extracted by a  $\text{H}_3\text{PO}_4$  acid technique with a VG-PRISM mass spectrometer. For the fracture-filling sample, three chips without coating (total weight 30 mg), with a few filled microfractures, were selected and leached with  $\text{H}_3\text{PO}_4$  acid for 12 hours, yielding about 0.3  $\mu\text{mol}$  of  $\text{CO}_2$ .
6. For the FEG-SEM observations and EDS chemical analyses, untreated samples with freshly exposed fractures were mounted on SPI carbon conductive adhesive tape followed by carbon coating with a Baltec modular high-vacuum coating system MED 020. The thickness of the carbon coating is difficult to estimate but is probably <15 nm. Operating conditions of the JEOL JSM6301-F microscope were 5 to 11 kV with a sample-to-objective working distance of 5 to 15 mm.
7. D. S. McKay *et al.*, *Science* **273**, 924 (1996).
8. J. P. Bradley *et al.*, *Nature* **390**, 454 (1997).
9. D. S. McKay *et al.*, *ibid.*, p. 455; R. A. Kerr, *Science* **278**, 1706 (1997).
10. R. L. Folk and F. L. Lynch, *J. Sediment. Res.* **67**, 583 (1997).
11. K. H. Nealson, *Annu. Rev. Earth Planet. Sci.* **25**, 403 (1997).
12. P. Gillet *et al.*, *Phys. Chem. Minerals* **20**, 1 (1993).
13. W. D. Bischoff *et al.*, *Am. Mineral.* **70**, 581 (1985); J. Urmos *et al.*, *ibid.* **76**, 641 (1991).
14. We are grateful to A. Carion and C. Perron (Musée National d'Histoire Naturelle) for generously donating the samples. We thank F. Albarède, P. Buseck, R. L. Folk, D. Rigomier, P. Thomas, P. Warren, and an anonymous reviewer for their constructive comments on the manuscript.

11 November 1997; accepted 20 February 1998

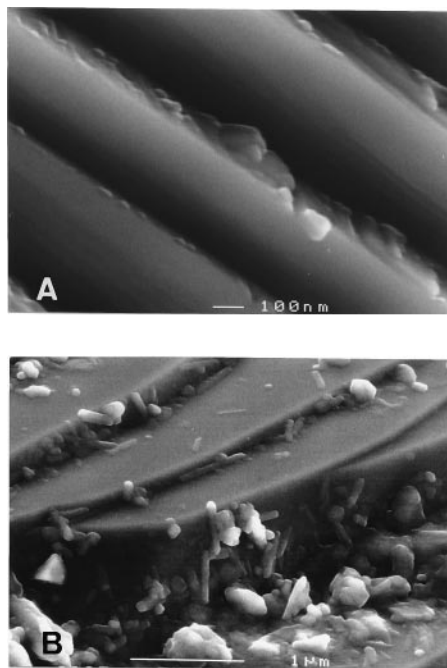


**Fig. 3.** Comparison of high-magnification FEG-SEM images of two pyroxene surfaces from the same Tatahouine sample. They were coated together on the same mount (6) to check for potential artifacts related to the coating procedures. (A) This surface was created by breaking the sample far away from any observed preexisting fractures. (B) This surface was near a rosette in a filled fracture. In both (A) and (B), the cleavages are observed. The rod-shaped forms are observed only in (B), ruling out a coating artifact for these features. Note also in (B) the random orientations of the rods.

## Oxygen Isotopic Abundances in Calcium-Aluminum-Rich Inclusions from Ordinary Chondrites: Implications for Nebular Heterogeneity

Kevin D. McKeegan,\* Laurie A. Leshin, Sara S. Russell, Glenn J. MacPherson

The oxygen isotopic compositions of two calcium-aluminum-rich inclusions (CAIs) from the unequilibrated ordinary chondrite meteorites Quinyambie and Semarkona are enriched in  $^{16}\text{O}$  by an amount similar to that in CAIs from carbonaceous chondrites. This may indicate that most CAIs formed in a restricted region of the solar nebula and were then unevenly distributed throughout the various chondrite accretion regions. The Semarkona CAI is isotopically homogeneous and contains highly  $^{16}\text{O}$ -enriched melilite, supporting the hypothesis that all CAI minerals were originally  $^{16}\text{O}$ -rich, but that in most carbonaceous chondrite inclusions some minerals exchanged oxygen isotopes with an external reservoir following crystallization.

CAIs in primitive chondrite meteorites are the oldest solid materials believed to have formed in the solar system (1, 2). Studies of their mineralogy, chemical composition,

K. D. McKeegan and L. A. Leshin, Department of Earth and Space Sciences, University of California Los Angeles, Los Angeles, CA 90095–1567, USA.

S. S. Russell and G. J. MacPherson, Department of Mineral Sciences, MRC NHB-119, National Museum of Natural History, Smithsonian Institution, Washington, DC 20560, USA.

\*To whom correspondence should be addressed. E-mail: kdm@ess.ucla.edu

and isotopic abundances have provided unique information regarding the thermal and chemical processing of materials during the earliest epoch of solar system formation (3). However, most previous studies examined CAIs from a relatively small group of meteorites (4), the carbonaceous chondrites (CCs), and most O isotopic measurements were restricted to only a few CCs that contain large and abundant CAIs. Thus, the extent to which inferences based on data from these CAIs can be generalized to the

solar nebula as a whole is not clear.

The genetic relationship, if any, between rare CAIs in the ordinary chondrites (OCs) and the more common CAIs in CCs will help elucidate chemical and isotopic distributions in the solar nebula and, by extension, thermal regimes and time scales of nebular processes. For example, Russell *et al.* (5) showed that the short-lived radionuclide  $^{26}\text{Al}$  was incorporated into two OC CAIs during their crystallization at  $\sim 5 \times 10^{-5}$  times the abundance of stable  $^{27}\text{Al}$ , the same level of enrichment of  $^{26}\text{Al}$  as found in most CAIs from CCs (6). Because the CCs and OCs are thought to have formed on planetesimals accreted at different heliocentric distances (7), this can be considered evidence that  $^{26}\text{Al}$  was originally present at this high initial abundance throughout extensive regions of the solar nebula (5). An alternative possibility is that most CAIs formed in a restricted region of the solar nebula, characterized by this high  $^{26}\text{Al}/^{27}\text{Al}$  ratio, and were subsequently dispersed throughout wide nebular regions including the OC and CC accretion zones. Oxygen isotopes can help resolve this issue.

The O isotopic compositions of solar system materials are unequilibrated on size scales ranging from microscopic to planetary [for review, see (8)]. The latter observation has served as a criterion for classifying meteorites into groups that each presumably originated on a separate asteroidal "parent body" (9, 10). On a three-isotope plot of  $\delta^{17}\text{O}$  versus  $\delta^{18}\text{O}$  (11), OC materials are characterized by O isotope compositions that lie above the slope  $1/2$  mass-dependent fractionation line defined by terrestrial and lunar samples (Fig. 1), whereas most CCs and their constituent phases (for example, CAIs, chondrules, and matrix) plot below the terrestrial fractionation (TF) line (8, 12). In particular, CAIs from CCs show variable degrees of  $^{16}\text{O}$ -enrichment (8, 13), extending to compositions with  $\delta^{18}\text{O} \approx \delta^{17}\text{O} \approx -40\%$ , and define a line with a slope close to unity [termed the carbonaceous chondrite anhydrous minerals line, or CCAM (Fig. 1) (13)]. The CCAM line cannot be produced by mass-dependent fractionation processes and has been explained as resulting from isotopic exchange between a reservoir of  $^{16}\text{O}$ -rich refractory dust and a second reservoir of more "normal" isotopic composition, most probably nebular gas (13–15). The O isotopic compositions of whole-rock OCs and their chondrules also define a slope  $\sim 1$  mixing line, extending above the TF line (that is,  $\Delta^{17}\text{O} > 0$ ) by a few per mil (10, 16). Like the CCAM line, this line represents mixtures of materials with different relative  $^{16}\text{O}$  abundances (10), but the degree of isotopic heterogeneity is less than that seen in CC minerals.

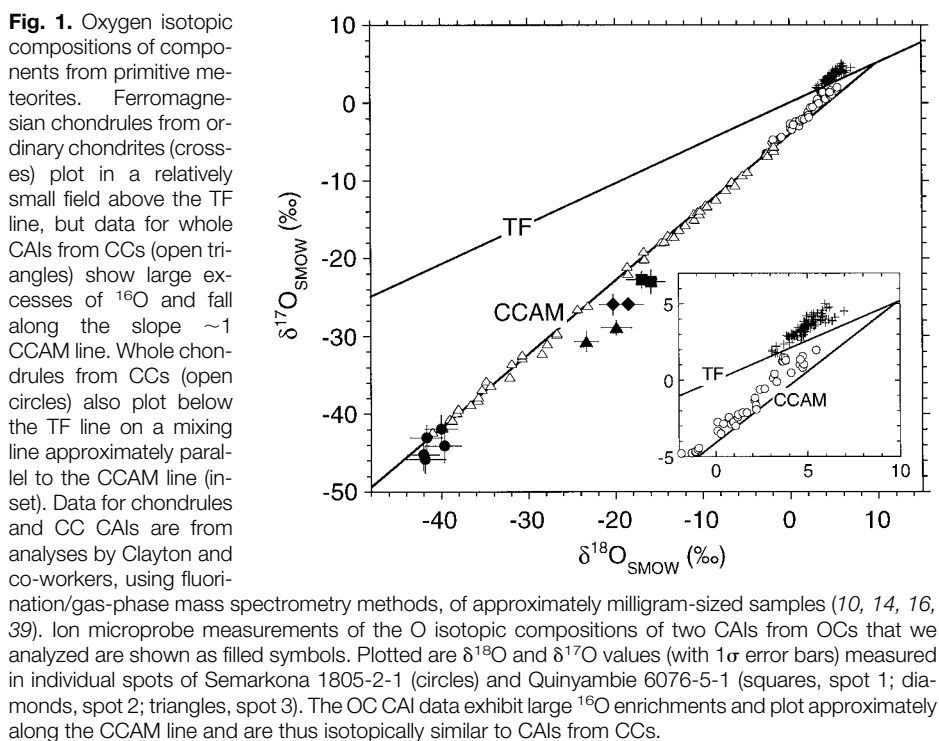
Because the O isotope compositions of the nebular accretion regions of the OCs and CCs are distinct (Fig. 1), the O isotopic compositions of CAIs from OCs could provide a means for assessing the provenance of these objects. CAIs from OCs are not only rare but also too small (3, 5) to be analyzed by conventional methods. The high sensitivity and localized analysis capability of the ion microprobe allowed us to measure the O isotopic composition in  $\sim 10$ - to  $12$ - $\mu\text{m}$  diameter spots of two CAIs from unequilibrated OCs (17).

The CAIs analyzed are the same two that were studied by Russell *et al.* (5): USNM 1805-2-1 from LL3.0 Semarkona and USNM 6076-5-1 from L3.4 Quinyambie (18). Semarkona 1805-2-1 is a lens-shaped inclusion,  $\sim 480$   $\mu\text{m}$  in longest dimension, that consists predominantly of densely intergrown crystals (mostly  $< 40$   $\mu\text{m}$  in size) of spinel, blue hibonite, and aluminum-rich melilite, with perovskite as a minor phase (3, 19). The inclusion is partially rimmed by a layered sequence of melilite surrounded by anorthite and then fassaite (3). Rare earth element (REE) abundances show a volatility-fractionated (group II) pattern (20) indicative of condensation from a gaseous reservoir that was depleted of the most refractory REEs (21). Melilite contains  $^{26}\text{Mg}$  excesses (5) at a level indicating  $(^{26}\text{Al}/^{27}\text{Al})_0 = (4.7 \pm 1.5) \times 10^{-5}$ . Quinyambie 6076-5-1 is a melilite-rich inclusion  $\sim 150$ - $\mu\text{m}$  long, consisting of several discontinuous nodules separated by Fe-rich fine-grained matrix material (5). Some of the nodules are rimmed

with Al-rich diopside, and grains of perovskite, hibonite, and spinel are enclosed within the melilite. Magnesium isotopic measurements (5) indicate  $(^{26}\text{Al}/^{27}\text{Al})_0 = (4.9 \pm 1.4) \times 10^{-5}$  of melilite and spinei.

Because both CAIs are fine-grained and had been extensively sputtered in previous ion probe studies (meaning that the choicest target areas were already destroyed), it was not possible to avoid analyzing mixtures of mineral phases even with a spatial resolution of  $\sim 10$   $\mu\text{m}$ . Therefore, following isotopic analysis, each sputtered crater was imaged in an electron microscope to determine the proportions of minerals sampled in the analysis (Table 1) (22). Two sets of O isotopic measurements were made on Quinyambie 6076-5-1 in order to assess reproducibility. The second ("B") set of measurements were intended to analyze material from the same craters as the first set, but some misalignment of the sample relative to the sputtering beam resulted in a slight enlargement of the crater (by  $< 5$   $\mu\text{m}$ ). Although the mixture of minerals analyzed in the second set may not be the same as in the first analysis, the data agree within analytical uncertainty in most cases.

Semarkona 1805-2-1 and Quinyambie 6076-5-1 are both enriched in  $^{16}\text{O}$  (Fig. 1) with O isotopic compositions that lie far from the fields previously defined by whole-rock OCs and their individual components such as chondrules (8, 10, 23). Semarkona 1805-2-1 shows the highest  $^{16}\text{O}$ -enrichments, with all five analysis spots plotting within error of the CCAM line in a region



characteristic of the maximum  $^{16}\text{O}$ -excesses measured in many CAIs from CCs (8, 14). In contrast to CAIs from type-3 CCs, in which O isotope compositions are correlated with mineralogy (8, 14, 24), the different minerals in Semarkona 1805-2-1 have the same isotopic compositions within our analytical uncertainties. Thus, the mineral distribution and isotopic data indicate that all minerals, including melilite, in this CAI must be  $^{16}\text{O}$ -enriched. Oxygen isotopic compositions of melilite mineral separates from CC CAIs invariably plot near the  $^{16}\text{O}$ -poor end of the CCAM line (14, 24, 25). However,  $^{16}\text{O}$ -rich melilite has been found by ion microprobe measurements of a CAI in the ungrouped chondrite ALH85085 (26) and in a micrometeorite collected from Antarctic ice (27).

While distinct from OC compositions, the data for Quinyambie 6076-5-1 are not as  $^{16}\text{O}$ -enriched as Semarkona 1805-2-1 and plot slightly to the high  $\delta^{18}\text{O}$  side of the CCAM line (Fig. 1). The presence of Fe-rich matrix material, which has an O isotopic composition in the OC field above the TF line (Fig. 1), in each analyzed spot of Quinyambie 6076-5-1 (Table 1) makes it difficult to accurately assess the bulk composition of the unaltered CAI and to distinguish the O isotopic compositions of individual minerals. However, because each spot analyzed in Quinyambie 6076-5-1 consists mostly of melilite plus this matrix material, in this sample the melilite must also be  $^{16}\text{O}$ -enriched. Finally, the position of the data to the high  $\delta^{18}\text{O}$  side of the CCAM line could be an instrumental artifact caused by the inclusion of Fe-rich material in the analysis (17).

The O isotope data have important implications for understanding the origins and subsequent processing of CAIs. The two or-

dinary chondrite CAIs so far analyzed yield levels of  $(^{26}\text{Al}/^{27}\text{Al})_0$  of  $\sim 5 \times 10^{-5}$  (5) and large  $^{16}\text{O}$ -excesses—both of which are typical properties of CAIs from CCs. Thus, bearing in mind the limited statistics, it appears that CAIs from OCs and CCs have the same distinctive isotopic characteristics, implying that they are genetically related.

The observation that the O isotopic compositions of two OC CAIs fall approximately along the CCAM line, and not on an extension of the line defined by other unequilibrated OC data (10), indicates that rare CAIs do not represent the  $^{16}\text{O}$ -rich end-member of the OC mixing line. Rather, CAIs from both CCs and OCs sampled an O isotope reservoir in the solar nebula that was distinct from that of typical OC materials.

If most CAIs crystallized nearly contemporaneously over a wide nebular volume (3, 5, 6), then our data indicate that the dust from which CAIs formed was approximately uniformly enriched in  $^{16}\text{O}$  in addition to  $^{26}\text{Al}$  in the accretion regions of CCs and OCs. In this case, the difference in inferred initial  $^{26}\text{Al}$  abundances between CAIs and chondrules in OCs would indicate different formation times, with CAIs crystallizing at least  $\sim 2$  million years before Al-rich and (presumably) ferromagnesian chondrules (5). However, the chondrules and other components that ultimately formed the OCs had different O isotopic compositions from not only the CAIs we analyzed, but also from their counterparts in the CC regions (10, 16). Thus, if the CAIs are representative of those nebular zones, then the O isotopic composition of these regions must have evolved subsequent to CAI formation. The differences between CC and OC chondrules (Fig. 1) would then require that the O iso-

topic composition of the nebula became increasingly heterogeneous with time, which is contrary to the expectation that progressive nebular evolution should tend to homogenize isotopic differences. One variant of the nebular evolution model postulates that the O isotopic composition of the nebula became more  $^{16}\text{O}$  depleted with time by incremental addition of relatively  $^{16}\text{O}$ -poor materials (28); however, this would imply that CC chondrules are older than OC chondrules, which is not supported by the  $^{26}\text{Al}$  data (5, 29).

Alternatively, if the nebula was isotopically heterogeneous on a large scale and on a grain-to-grain scale, then CAIs could have formed from a unique  $^{16}\text{O}$ -rich variety of precursor dust that was widely distributed throughout many nebular zones, while other components (for example, chondrule precursors) varied isotopically from zone to zone. In this case, it is difficult to understand how CAIs everywhere could maintain their unique O isotopic signatures since trace element fractionation patterns suggest that many CAIs [including Semarkona 1805-2-1 (20, 21)] are the result of a complex history of volatilization and recondensation (3) which would result in isotopic equilibration with surrounding materials.

Although none of the above models in which CAIs are made over wide nebular regions can be ruled out, the O isotopic data are suggestive of a different scenario in which all CAIs were formed in the same restricted nebular locale and were later distributed (in unequal abundances) to the nebular regions where the different chondrite groups eventually accreted. This general approach is capable of explaining why CAIs from OCs are isotopically similar to CAIs from CCs, but are so different in O isotopic composition from other phases in OC meteorites.

One recently proposed model for local formation of CAIs (30) links the petrogenesis of CAIs and chondrules to localized high-energy environments near the protosun ( $\sim 0.06$  astronomical units) and simultaneously provides a natural transport mechanism, in the form of bipolar outflows, for scattering these materials out to large radial distances in the accretion disk where they may later be incorporated into parent asteroids of chondrites. The model also suggests that  $^{26}\text{Al}$  may have been produced in the same near-solar region by particle irradiation, although this aspect has been criticized because of problems of over-production of other short-lived nuclides (31). Although the data presented here are generally supportive of this type of model because of its spatially restricted formation region for all CAIs, there are other problems with this particular model in terms of explaining

**Table 1.** Oxygen isotopic compositions of ordinary chondrite CAIs.

Location	$\delta^{18}\text{O}$ (‰)	$\delta^{17}\text{O}$ (‰)	$\Delta^{17}\text{O}$ (‰)	Approximate mineralogy* (volume %)
<i>Semarkona 1805-2-1</i>				
Spot 1	$-41.8 \pm 2.4$	$-45.8 \pm 1.8$	$-24.0 \pm 2.1$	Sp (74), Mel (16), Pv (10)
Spot 2	$-40.0 \pm 1.8$	$-41.9 \pm 1.8$	$-21.1 \pm 2.0$	Sp (39), Hib (39), Mel (18), + Pv
Spot 3	$-41.7 \pm 1.8$	$-43.0 \pm 1.6$	$-21.4 \pm 1.9$	Sp (57), Mel (43)
Spot 4	$-42.0 \pm 1.8$	$-45.2 \pm 2.0$	$-23.4 \pm 2.2$	Sp (93), Mel (7)
Spot 5†	$-39.7 \pm 1.9$	$-44.1 \pm 2.1$	$-23.5 \pm 2.3$	Mel (55), An (27), Sp (18)
<i>Quinyambie 6076-5-1</i>				
Spot 1	$-16.9 \pm 1.8$	$-22.7 \pm 1.1$	$-13.9 \pm 1.2$	Mel (77), Mx (18), + Sp, Pv
Spot 1B	$-15.8 \pm 1.6$	$-23.0 \pm 1.5$	$-14.8 \pm 1.6$	
Spot 2	$-18.5 \pm 1.7$	$-25.9 \pm 0.8$	$-16.3 \pm 1.0$	Mel (69), Mx (27), + Sp, Pv
Spot 2B	$-20.2 \pm 1.5$	$-25.9 \pm 1.3$	$-15.4 \pm 1.4$	
Spot 3	$-19.8 \pm 1.7$	$-28.9 \pm 0.9$	$-18.6 \pm 1.1$	Mel (69), Sp (16), Mx (12), + Pv
Spot 3B	$-23.3 \pm 1.3$	$-30.7 \pm 1.3$	$-18.6 \pm 1.3$	

\*Approximate mineralogical composition of each analyzed spot is listed in terms of decreasing abundance. The volume % of each mineral's contribution to the isotopic analysis was estimated by electron microscope imaging or point count analysis of the sputtered crater, assuming comparable sputter rates for each mineral. Phases detected at minor abundance (<5%) are just noted; Quinyambie spot 3 also contained <5 volume % of cracks. Accuracy of estimate is probably  $\sim 20\%$  relative. An, anorthite; Hib, hibonite; Mel, melilite; Pv, perovskite; Sp, spinel; Mx, matrix. †Semarkona spot 5 was located near the rim of the inclusion; all other analysis points were from the inclusion interior. Spot locations in Quinyambie were from interior points on different nodules separated by fine-grained Fe-rich matrix.

many of the characteristics of chondrules. For example, it is not clear how the model can account for the O isotopic differences between chondrules in OCs and CCs. Additionally, some Al-rich chondrules in OC contain detectable excesses of  $^{26}\text{Mg}$  attributable to decay of  $^{26}\text{Al}$  (5), yet they have O isotope signatures related to those of their host parent meteorites and different from those of CAIs (32). In summary, we conclude that some variant of the local formation model for CAIs is most appealing for explaining their O isotopic compositions because it is the simplest and requires the fewest ad hoc assumptions. However, it remains to be seen if further development of the specific model discussed above (30) can address all the relevant observations of chondrules and CAIs, or if some other scenario for formation of CAIs in a restricted nebular locale can better explain the data.

If correct, a scenario in which CAIs are produced in a restricted region of the accretion disk conceivably weakens the argument that the initial  $^{26}\text{Al}/^{27}\text{Al}$  values of refractory inclusions are representative of the isotopic composition of the entire nebula. Thus, it may not be warranted to infer relative chronologies of CAIs and chondrules based on relative abundances of initial  $^{26}\text{Al}$ , although the implications derived from the distribution of initial  $^{26}\text{Al}$  in CAIs for duration of the solar nebula could still be valid (5, 6, 33). However, because the processes and locations of CAI and chondrule formation are still poorly constrained, it may be premature to conclude that CAIs, even if locally produced, are not representative of the nebular isotopic composition of aluminum at the time of their formation (5, 6).

In type B CAIs from CCs, O isotopes are heterogeneously distributed on a microscopic scale such that spinel and pyroxene are  $^{16}\text{O}$  enriched compared to melilite and anorthite (14, 24, 25). The gas-solid isotopic exchange model explains this by postulating that CAIs first solidified with a uniform enrichment of  $^{16}\text{O}$  in all mineral phases, and some inclusions then partially exchanged their initial O with that of nebular gas (15). In this model, the extent of isotopic exchange is dependent on the O diffusivity in each mineral phase and the temperature history of the CAI. Difficulties with this general model have been in quantitatively reconciling laboratory-measured diffusion rates with meteoritic compositions (34) and the absence of direct observations of the postulated unexchanged CAIs. The isotopic homogeneity of Semarkona 1805-2-1 resolves the latter problem and thus supports the hypothesis that all CAI minerals were originally  $^{16}\text{O}$  enriched.

## REFERENCES AND NOTES

1. F. A. Podosek *et al.*, *Geochim. Cosmochim. Acta* **55**, 1083 (1991); J. H. Chen and G. J. Wasserburg, *Earth Planet. Sci. Lett.* **52**, 1 (1981).
2. G. R. Tilton, in *Meteorites and the Early Solar System*, J. F. Kerridge and M. S. Matthews, Eds. (Univ. of Arizona Press, Tucson, 1988), pp. 259–275.
3. G. J. MacPherson, D. A. Wark, J. T. Armstrong, in (2), pp. 746–807.
4. The great majority (~80%) of primitive, undifferentiated meteorites observed to fall are classified as ordinary chondrites, whereas the more volatile-rich carbonaceous chondrites constitute <5% of observed falls.
5. S. S. Russell, G. Srinivasan, G. R. Huss, G. J. Wasserburg, G. J. MacPherson, *Science* **273**, 757 (1996).
6. G. J. MacPherson, A. M. Davis, E. K. Zinner, *Meteoritics* **30**, 365 (1995).
7. D. W. G. Sears and R. T. Dodd, in (2), pp. 3–31.
8. R. N. Clayton, *Annu. Rev. Earth Planet. Sci.* **21**, 115 (1993).
9. R. N. Clayton and T. K. Mayeda, *Earth Planet. Sci. Lett.* **40**, 168 (1978); R. N. Clayton, N. Onuma, T. K. Mayeda, *ibid.* **30**, 10 (1976); R. N. Clayton and T. K. Mayeda, *ibid.* **62**, 1 (1983).
10. R. N. Clayton, T. K. Mayeda, J. N. Goswami, E. J. Olsen, *Geochim. Cosmochim. Acta* **55**, 2317 (1991).
11. Oxygen isotopic compositions are expressed as delta-values, the deviation in per mil relative to a standard composition (standard mean ocean water, or SMOW)
 
$$\delta^{18}\text{O} = \left( \frac{^{18}\text{O}/^{16}\text{O}_{\text{sample}}}{^{18}\text{O}/^{16}\text{O}_{\text{SMOW}}} - 1 \right) \times 1000$$
 and similarly for  $\delta^{17}\text{O}$ . The deviation of the O isotopic composition from the terrestrial fractionation line is expressed by  $\Delta^{17}\text{O}$ , where  $\Delta^{17}\text{O} = \delta^{17}\text{O} - 0.52\delta^{18}\text{O}$
12. The principal exception to this observation is the aqueously altered CI chondrites. [M. W. Rowe, R. N. Clayton, T. K. Mayeda, *Geochim. Cosmochim. Acta* **58**, 5341 (1994); L. A. Leshin, A. E. Rubin, K. D. McKeegan, *ibid.* **61**, 835 (1997)].
13. R. N. Clayton, L. Grossman, T. K. Mayeda, *Science* **182**, 485 (1973).
14. R. N. Clayton, N. Onuma, L. Grossman, T. K. Mayeda, *Earth Planet. Sci. Lett.* **34**, 209 (1977).
15. R. N. Clayton and T. K. Mayeda, *Geophys. Res. Lett.* **4**, 295 (1977); M. Blander and L. H. Fuchs, *Geochim. Cosmochim. Acta* **39**, 1605 (1975).
16. R. N. Clayton *et al.*, in *Chondrules and Their Origins*, E. A. King, Ed. (Lunar and Planetary Institute, Houston, TX, 1983), pp. 37–43.
17. The ion microprobe requires only small sample amounts (less than ~2 ng) for a determination of O isotope composition (35, 36). We used the Cameca IMS 1270 ion microprobe at the University of California, Los Angeles, to perform O isotopic measurements by sputtering polished, C-coated thin sections with a 20-keV, ~0.3-nA Cs<sup>+</sup> beam defocused to produce a uniformly illuminated spot of about 10  $\mu\text{m}$  diameter at the sample surface. This configuration results in the formation of a shallow (<2  $\mu\text{m}$ ) flat-bottomed crater during the analysis time (~20 min). Low-energy (0 to ~30 eV) negative secondary ions were accelerated to 10 keV and mass analyzed at high resolving power ( $m/\Delta m > 6500$ ) in order to separate interfering molecular species ( $^{16}\text{OH}^-$ ,  $^{17}\text{OH}^-$ ,  $^{16}\text{OH}_2^-$ ) from atomic O ions. A normal-incidence electron gun was used to flood the analysis area with low-energy electrons for charge compensation (37). The  $^{17}\text{O}^-$  count rate was corrected for possible tailing of the intense  $^{16}\text{OH}^-$  peak; these corrections were always <0.5%, and typically <0.2%, in  $\delta^{17}\text{O}$ . A Faraday cup (FC) detector (equipped with a Keithley 642 electrometer) was used to measure the intense  $^{16}\text{O}^-$  current ( $20 \times 10^6$  to  $30 \times 10^6$  ions per second equivalent), whereas the ion beams for the minor isotopes  $^{17}\text{O}$  and  $^{18}\text{O}$  were measured by pulse counting with an electron multiplier (EM). Ion intensities were corrected for background (FC) and deadtime (EM); both corrections are small at these count rates and can be made with an accuracy better than ~0.1%. The raw O isotope ratios were corrected for instru-
18. The CAI Quinyambie 6076-5-1 was previously (5) given the name Moorabie, because these two meteorites were initially believed to be paired (38) and the name Moorabie was assigned to the pairing group. The pairing is now in doubt and so the name Quinyambie will be used for this object.
19. A. Bischoff and K. Keil, *Geochim. Cosmochim. Acta* **48**, 693 (1984).
20. A. J. Fahey, thesis, Washington University, St. Louis, MO (1988).
21. W. V. Boynton, *Geochim. Cosmochim. Acta* **39**, 569 (1975).
22. The mineralogy sampled by the ion probe beam was determined by point counting and image analysis of backscattered electron photographs of the craters. Errors due to counting statistics are between 10 and 20% relative.
23. J. M. Saxton, I. C. Lyon, G. Turner, *Meteoritics* **30**, 571 (1995).
24. K. D. McKeegan, L. A. Leshin, S. S. Russell, G. J. MacPherson, *Meteoritics Planet. Sci.* **31**, A86 (1996).
25. T. K. Mayeda, R. N. Clayton, H. Nagasawa, *Lunar Planet. Sci.* **XVII**, 526 (1986).
26. M. Kimura, A. El Goresy, H. Palme, E. Zinner, *Geochim. Cosmochim. Acta* **57**, 2329 (1993).
27. C. Engrand, K. D. McKeegan, L. A. Leshin, *Meteoritics Planet. Sci.* **32**, A39 (1997).
28. B.-G. Choi and J. T. Wasson, *ibid.*, p. A28.
29. Y. J. Sheng, I. D. Hutcheon, G. J. Wasserburg, *Geochim. Cosmochim. Acta* **55**, 581 (1991).
30. F. H. Shu, H. Shang, T. Lee, *Science* **271**, 1545 (1996).
31. J. N. Goswami, K. K. Marhas, S. Sahajpal, *Lunar Planet. Sci.* **XXVIII**, 349 (1997).
32. S. S. Russell, L. A. Leshin, K. D. McKeegan, G. J. MacPherson, *Meteoritics Planet. Sci.* **32**, A111 (1997).
33. F. A. Podosek and P. Cassen, *Meteoritics* **29**, 6 (1994).
34. F. J. Ryerson and K. D. McKeegan, *Geochim. Cosmochim. Acta* **58**, 3713 (1994).
35. K. D. McKeegan, *Science* **237**, 1468 (1987).
36. J. W. Valley, C. M. Graham, B. Harte, J. M. Eiler, P. D. Kinny, in *Applications of Microanalytical Techniques to Understanding Mineralizing Processes*, vol. 7 of *Society of Economic Geology Reviews in Economic Geology*, M. A. McKibben, W. C. Shanks, W. I. Ridley, Eds. (Economic Geology Publishing, El Paso, TX, in press).
37. G. Slodzian, M. P. Chaintreau, R. C. Dennebouy, in

Cameca News (Cameca Instruments Inc., Trumbull, CT, 1987), pp. 1–6.

38. A. L. Graham, A. W. R. Bevan, R. Hutchison, *Catalogue of Meteorites* (Univ. of Arizona Press, Tucson, AZ, 1985).
39. R. N. Clayton, T. K. Mayeda, J. N. Goswami, E. J. Olsen, *Terra Cognita* 6, 130 (1986).

40. We gratefully acknowledge the laboratory assistance of C. Coath, C. Engrand, and G. Jarzebinski. The manuscript was improved by constructive comments from two anonymous reviewers. Supported by NASA grants NAG5-4704 (K.D.M.) and NAGW-3553 (G.J.M.).

9 October 1997; accepted 3 March 1998

## Osmium Isotopic Evidence for Ancient Subcontinental Lithospheric Mantle Beneath the Kerguelen Islands, Southern Indian Ocean

Deborah R. Hassler and Nobumichi Shimizu

Upper mantle xenoliths found in ocean island basalts are an important window through which the oceanic mantle lithosphere may be viewed directly. Osmium isotopic data on peridotite xenoliths from the Kerguelen Islands, an archipelago that is located on the northern Kerguelen Plateau in the southern Indian Ocean, demonstrate that pieces of mantle of diverse provenance are present beneath the Islands. In particular, peridotites with unradiogenic osmium and ancient rhenium-depletion ages (to  $1.36 \times 10^9$  years old) may be pieces of the Gondwanaland subcontinental lithosphere that were incorporated into the Indian Ocean lithosphere as a result of the rifting process.

The Kerguelen hotspot became active at least 115 million years ago (Ma) (1), and possibly as long as 130 Ma, when India separated from Australia-Antarctica (2). The Kerguelen mantle plume is considered to be responsible for extensive hotspot volcanism in the Indian Ocean basin (3), including the Ninetyeast Ridge, Broken Ridge, and the Kerguelen Plateau, the second largest of the oceanic plateaus (Fig. 1). Moreover, the Kerguelen plume is a carrier of the DUPAL isotopic anomaly (4), a characteristic of basalts erupted in the Southern Hemisphere. The interaction of this plume with the Indian Ocean lithosphere has potentially affected the geochemical and tectonic evolution of the entire Indian Ocean basin (2, 5).

One notion for the origin of the Kerguelen Plateau and the Kerguelen Islands is that their lithospheric basement contains a continental fragment left behind from the breakup of Gondwanaland (6). Basalts from the southern Kerguelen Plateau (Ocean Drilling Project drill site 738) do have trace element and isotopic signatures indicative of a continental component in their source (7), and recent seismic experiments showed that the southern Kerguelen Plateau has a structure similar to that of a continental passive margin (8). However, a seismic refraction

D. R. Hassler, Massachusetts Institute of Technology-Woods Hole Oceanographic Institution, Joint Program in Oceanography, Department of Geology and Geophysics, Woods Hole Oceanographic Institution, Woods Hole, MA 02543, USA.  
N. Shimizu, Department of Geology and Geophysics, Woods Hole Oceanographic Institution, Woods Hole, MA 02543, USA.

study, as well as early isotopic work on basalts from the archipelago, established an apparent oceanic origin (6, 9). Here we present Os isotopic data that establish the presence of continental lithosphere in the northern Kerguelen Plateau and the involvement of continental materials in the formation of the Kerguelen Islands.

We examined the Re-Os isotopic systematics in peridotite xenoliths (10) from two

sample localities that are less than 10 km apart (Lac Superieur and Mont Trapeze) in the Courbet Peninsula, northeastern Kerguelen Islands (Fig. 1, inset). The xenoliths are abundant in alkaline basaltic dikes that cross-cut "plateau basalt" lavas that comprise the Courbet Peninsula and formed 23 to 25 million years ago (Ma) (11).

The samples are predominantly refractory coarse granular harzburgites [olivine: ~60% (forsterite content = 90 to 92%); orthopyroxene: ~35%; clinopyroxene: 1 to 5%; and trace amounts of spinel], but also include more clinopyroxene-rich lherzolites and wehrlitic-dunites. The rocks are fresh and do not contain any secondary alteration minerals. Many of the peridotites (from both localities) reacted with melts that percolated through them. For example, some harzburgites contain newly formed clinopyroxene crystals that are enriched in incompatible trace elements (for example, chondrite normalized  $La_N = 100$ ), whereas coexisting original clinopyroxene grains occur as symplectite intergrowths with both orthopyroxene and spinel and have depleted incompatible trace element abundances (for example,  $La_N = 3$ ). Some peridotites at more advanced stages of reaction have trace element-enriched clinopyroxenes (for example,  $La_N = 300$ ) that are intergrown with phlogopite (12).

During interactions with percolating metasomatic melts, the Sr and Nd isotopic characteristics of the original peridotites are likely to be replaced by those of the melt, because the concentrations of these incom-

**Table 1.** Rhenium and osmium isotopic results from Kerguelen Islands peridotite xenoliths. All samples are spinel harzburgites except as noted. ND, not determined.

Sample	$^{187}\text{Os}/^{188}\text{Os}$	Os (33) (ppt)	Re (ppt)	Re/Os ( $\times 10^{-3}$ )	$T_{\text{RD}}$ (25) (Ga)
<i>Lac Superieur</i>					
OB93-51*	0.1262 ± 2	87	ND		
OB93-52†	0.1286 ± 3	4218	ND		
OB93-64‡	0.1300 ± 2	968	ND		
OB93-77	0.1263 ± 3	3199	5	2	
OB93-78	0.1266 ± 6	2888	ND		
OB93-80	0.1252 ± 2	1727	ND		
OB93-82‡	0.1287 ± 2	6999	ND		
OB93-83*§	0.1257 ± 4	44	ND		
<i>Mont Trapeze</i>					
OB93-280	0.1189 ± 2	3067	6	2	1.36
OB93-284	0.1236 ± 1	6652	29	4	0.63
OB93284b	0.1229 ± 3	6645	ND		0.74
OB93-287	0.1239 ± 3	1267	49	39	0.58
OB93-289	0.1224 ± 3	3411	12	4	0.81
OB93-291	0.1205 ± 4	2157	11	5	1.11
OB93-297	0.1228 ± 3	2409	31	13	0.75
OB93-305	0.1211 ± 3	2012	72	36	1.02
OB93-305r	0.1202 ± 4	2179	ND		1.16
OB93-306	0.1276 ± 5	516	41	80	
OB93-307	0.1229 ± 3	5605	49	9	0.74
OB93-314	0.1383 ± 6	3281	9	3	
OB93-317	0.1196 ± 4	2652	11	4	1.25

\*Olivine separate. †Spinel lherzolite. ‡Wehrlitic dunite. §Phlogopite-bearing spinel lherzolite. ||Replicate.